

# Caputo fractional-time of a modified Cahn-Hilliard equation for the inpainting of binary images

Anouar Ben-loghfry<sup>†\*</sup>, Abdelilah Hakim<sup>‡</sup>

<sup>†</sup>*Department of mathematics, Faculty of Sciences and Technologies Mohammedia, University Hassan II, Casablanca, Morocco*

<sup>‡</sup>*LAMAI laboratory, university of Cadi Ayyad, Faculty of sciences and technology, Marrakesh, Morocco*

*Email(s): anwarbenloghfry@gmail.com, abdelilahhakim@gmail.com*

---

**Abstract.** In this work, we present a new version of the Cahn-Hilliard equation to deal with binary image inpainting. The proposed model is unique due to its memory effect ability implemented by the time fractional derivative. Also, this model has a new diffusion term that gives a topological reconnection and a well sharpness of edges and corners. We give an existence result with some numerical tests implemented by the convexity splitting to show the efficiency of the proposed model.

*Keywords:* Image inpainting, Cahn-Hilliard equation, time-fractional, Caputo derivative, finite difference, convexity splitting.

*AMS Subject Classification 2010:* 58F15, 58F17, 53C35.

---

## 1 Introduction

Image inpainting is the process of recovering clean data from a damaged image. In other words, image inpainting is to restore a damaged observed image with missing information. It has many interesting fields of applications, such as medical imaging, photoshop, augmented reality, robotic, etc (for more see [9, 10, 25, 39]). In literature, different models have been dealing with image inpainting with different validations and successes. For instance, we mention partial differential equations (PDEs) [39], which are widely used and showed remarkable results, especially for cartoon and binary images. In this work, we are interested in applying the modified Cahn-Hilliard equation for inpainting binary images [18]. It was invented to describe the evolution of an interface between two state phases. The Cahn-Hilliard equation is a fourth-order semi-linear PDE which is derived from the  $H^1$ -gradient flow of the following

---

\*Corresponding author

Received: 27 March 2022 / Revised: 14 April 2023 / Accepted: 16 April 2023

DOI: 10.22124/jmm.2023.22019.1938

Ginzburg-Landau energy:

$$\frac{1}{2} \int_{\Omega} |\nabla u|^2 + \frac{F(u)}{\varepsilon^2} dx,$$

where  $F(u) = \frac{1}{2}u^2(1-u)^2$  is a smooth free energy Elliott [24] called double-well potentials. For binary image inpainting, Cahn-Hilliard equation was first exploited by Bertozzi et al. [11, 13] by the following (modified) version (stationary):

$$-\Delta \left( \Delta u - \frac{1}{\varepsilon^2} F'(u) \right) + \lambda(f - u) = 0, \quad \text{in } \Omega. \quad (1)$$

Eq. (1) is obtained by including the fidelity part  $\lambda(f - u)$ , where  $f$  is the observed data in the damaged subdomain  $\Omega \setminus D$  (inpainting region), and

$$\lambda(x) = \lambda_0 \chi_{\Omega \setminus D},$$

where  $\lambda > 0$  is set to balance the fidelity term and the state phase, and  $\chi_{\Omega \setminus D}$  is the known indicator function of the subdomain  $\Omega \setminus D$ . The two state-phases  $F$  introduced by the Cahn-Hilliard equation play a big role in homogeneous regions, while the interface between them plays the role on the edges and the corners. The reason refers to the double well potential  $F$  which vanishes only at the values of 0 and 1. The model (1) is only proposed for inpainting binary images (two-scale). In the literature, other generalizations from binary images to grayscale and colored images have been proposed [17, 21, 22, 27, 42]. The feature quality of Cahn-Hilliard is related to the choice of the parameter  $\varepsilon > 0$ , which is usually clear near sharp edges and corners. Indeed, taking a large value of  $\varepsilon$  is always needed in order to join edges over large distances. On the other hand, a small value of  $\varepsilon$  is needed to obtain the preservation of sharp edges and also for the other features. Moreover, choosing  $\varepsilon$  to be constant (large or small) is not practical. In other words, it is not relevant to recover damaged areas due to the balance between inpainting of areas and sharpening of edges at the same time [11–13]. To remedy this issue, the authors in [11, 12] proposed to use a procedure with two steps. The first step starts the simulation of the numerical computation with a large value of  $\varepsilon$  to reach a steady state. Next, the second step uses a new system with a small value of  $\varepsilon$  using the previous result with the big value of  $\varepsilon$ , as initial data in order to sharpen and preserve the features, such as edges and corners. In this work, we are interested in studying the following modified Cahn-Hilliard equation with a fractional-time order derivative:

$$\begin{aligned} \frac{\partial^\alpha u}{\partial t} &= -\varepsilon \nabla^2 \cdot (\Delta_{\mathcal{A}} u) + \frac{1}{\varepsilon} \Delta(F'(u)) + \lambda_D(f - u), & \text{in } \Omega \times (0, T), \\ u(x, 0) &= f(x), & \text{on } \Omega \setminus D, \\ \nabla u &= \nabla f, & \text{on } \partial D, \end{aligned} \quad (2)$$

where  $\Omega \subset \mathbb{R}^2$ , a bounded domain with  $D \subset \Omega$  the damage (inpainting) domain,  $T, \varepsilon > 0$ ,  $f \in L^2(\Omega)$  is the observed image with the damaged part,  $\lambda_D = \lambda \chi_{\Omega \setminus D}$  where  $\chi_{\Omega \setminus D}$  is the indicator function,  $F(u) = u^2(1-u)^2$  is a smooth free energy Elliott [14, 15],  $\Delta_{\mathcal{A}} u = \mathcal{A}_u \nabla^2 u$  is the diffusion term to control the amount of the smoothing and regularity of the operator and finally  $\frac{\partial^\alpha u}{\partial t}$  is the time-fractional  $\alpha$ -order derivative in the sense of Caputo [34]. We will explicitly introduce every term in the next section.

Now, we focus on justifying the modeling choices of our proposed model (2). The fractional derivative in the sense of Caputo is used in order to benefit from its potential of memory effect. This later was studied

in [3, 5–8, 23, 28, 37], where the authors proposed a system of fractional differential equations to study the effect of memory on epidemic evolution equations. Furthermore, one type of memory effect, which is extensively observed in ecology and epidemiology, was hysteresis. In hysteresis, the current state of the system depends on the current conditions and also on the previous ones, which means that the current event is influenced by the past systems [4, 20, 41]. In [35], the hysteresis potential is included in biological models because the defense mechanism of some living creatures is activated. For instance, in a situation of disease spreading (human beings), the vaccine can have a long-term memory potential, when it has a lasting effect, leaving the body to defend itself thanks to its immune memory system. Biologists and mathematicians have concluded that the best tool for modeling those kind of problems refers to the use of fractional Caputo derivative [5, 7, 8, 19, 31]. Mathematically speaking, a fractional-order derivative over time of an image  $u$  can be seen as a weighted sum of the successive terms  $u(x, t_0)$ ,  $u(x, t_1)$ ,  $u(x, t_N)$ , where  $t_0, \dots, t_N$  are the time steps. The fractional derivative explicitly uses the old versions of the observed image until it converges to the perfect and desired final image, contrarily to the classical derivative.

### Our contributions

In this paper, we articulate the following contributions:

- We incorporate the time-fractional derivative tool to improve the visual results. Thanks to the memory effect employed by the fractional Caputo derivative, we ensure sharpness of edges and features. Using the diffusion term, we guarantee an insightful inpainting process for the damaged domain in the final clean binary image.
- We investigate the existence result of our model, using Schauder fixed-point theorem with some new compactness results in the fractional case.
- We apply thorough discretization with a finite difference scheme, by introducing the proposed two steps procedure [11, 12] as mentioned above, with the convexity splitting method.
- We enrich our modeling with some rigorous numerical simulations with discussions and comparisons.

The structure of this paper is as follows, Section 2 deals with the theoretical results of our model (2). In Section 3, we discuss the discretization of our approach and we give some visual results next to some detailed remarks. Finally, we brief with a conclusion in Section 4.

## 2 Our approach and some tools

In this section, we start by explicitly introducing our model. First, we rewrite our model (2) as follows

$$\begin{aligned}
 \frac{\partial^\alpha u}{\partial t} &= -\varepsilon \nabla^2 (\Delta_{\mathcal{A}} u) + \frac{1}{\varepsilon} \Delta (F'(u)) + \lambda_D (f - u), & \text{in } \Omega \times (0, T), \\
 u(x, 0) &= f(x), & \text{on } \Omega \setminus D, \\
 \nabla u &= \nabla f, & \text{on } \partial D.
 \end{aligned}
 \tag{3}$$

The time-fractional derivative utilized is in the sense of Caputo and it has the following form:

$$\frac{\partial^\alpha u(t, x)}{\partial t} = \frac{1}{\Gamma(1-\alpha)} \int_0^t \frac{\partial u}{\partial \tau}(\tau, x) \frac{1}{(t-\tau)^\alpha} d\tau, \quad 0 < \alpha < 1.$$

The term  $\mathcal{A}_u$  in  $\Delta_{\mathcal{A}} u = \mathcal{A}_u \nabla^2 u$  is an anisotropic diffusion matrix which its main role is to control the smoothing process. Moreover,  $\mathcal{A}_u := \mathcal{A}_u(J_\rho(\nabla u_\sigma))$  depends on its structure  $J_\rho$ . It is defined by

$$J_\rho(\nabla u_\sigma) = G_\rho * (\nabla u_\sigma \otimes \nabla u_\sigma) = G_\rho * (\nabla(G_\sigma * u) \otimes \nabla(G_\sigma * u)^t),$$

where  $G_\rho$  and  $G_\sigma$  are two Gaussian convolution kernels, having the following form  $G_\tau = \frac{1}{2\pi\tau^2} \exp(-\frac{|x|^2}{2\tau^2})$ . The diffusion tensor  $\mathcal{A}_u$  is computed using the eigenvalues and the eigenvectors of the structure tensor  $J_\rho$ . Its purpose is to encode different scales in the image. In order to define the diffusion tensor  $\mathcal{A}_u$ , we consider an eigenvalue decomposition  $J_\rho(x) = V^T(x)\Sigma(x)V(x)$ , where  $V(x) \in \mathbb{R}^{2 \times 2}$  is an orthogonal matrix and  $\Sigma(x) := \text{diag}(\lambda_+(x), \lambda_-(x)) \in \mathbb{R}^{2 \times 2}$  is the diagonal matrix of the ordered eigenvalues, where  $\lambda_{+/-}$  are the the eigenvalues of the tensor structure  $J_\rho$ . Those eigenvalues can be calculated as follow:

$$\lambda_{+/-} = \frac{1}{2} \left( \text{trace}(J_\rho) \pm \sqrt{\text{trace}^2(J_\rho) - 4\det(J_\rho)} \right).$$

The diffusion tensor  $\mathcal{A}_u$  is defined by

$$\begin{aligned} \mathcal{A}_u : \Omega &\rightarrow \text{Sym}^2 \\ x &\mapsto V^T(x) \text{diag}(\theta(\lambda_+(x) - \lambda_-(x)), 1) V(x), \end{aligned}$$

where  $\text{Sym}^2$  is the set of symmetric matrices in  $\mathbb{R}^{2 \times 2}$  and

$$\theta(s) := \frac{1}{1 + \frac{s^2}{\theta_0}},$$

for some threshold  $\theta_0 > 0$ .

The  $\mathcal{A}_u$  is justified using geometric characteristics. Indeed, if  $\lambda_{+/-} \approx 0$ , the smoothing will be held in homogeneous areas which will be isotropic. While if  $\lambda_+ \gg \lambda_- \approx 0$  or  $\lambda_- \gg \lambda_+ \approx 0$ , the smoothing process is anisotropic and oriented along the edges, which is our main interest in recovering the damaged domain. However, if  $\lambda_+ \gg \lambda_- \gg 0$ , the smoothing goes into corners (junctions of edges). For the function  $\theta$ , it is also chosen to satisfy the above constraints.

## 2.1 Preliminaries

In this section, we give some useful results to show the well-posedness of our model (3). Firstly, we give the following assumptions for the diffusion matrix  $\mathcal{A}_u$ :

(H1)  $\mathcal{A}_u$  is Lipschitz in  $\mathcal{C}^1(\mathbb{R})$ , bounded and coercive,

(H2)  $\mathcal{A}_u$  is a symmetric positive-definite matrix.

Secondly, we give some useful definitions of the fractional calculus and the connection between some derivatives utilized in this paper. Additionally,  $AC([a, b])$  is the space of functions which are absolutely continuous on  $[a, b]$  and  $AC^n([a, b])$  ( $n \in \mathbb{N}_0$ ) is the space of functions  $f$  such that  $f' \in C^{n-1}([a, b])$  and  $f^{(n-1)} \in AC([a, b])$ . In particular,  $AC^1([a, b]) = AC([a, b])$ . To simplify, we take a function  $f$  in one dimensional space, defined in  $[a, b]$ , where  $f \in AC^n([a, b])$  and  $\alpha \in [n - 1, n)$ .

**Definition 1** ([30, 36]). *The left fractional derivative in the sense of Riemann-Liouville  $D_{[a,x]}^\alpha f(x)$  of order  $\alpha \in \mathbb{R}_+$ , is defined by*

$$D_{[a,x]}^\alpha f(x) = \frac{d^n}{dx^n} D_{[a,x]}^{-(n-\alpha)} f(x) = \frac{1}{\Gamma(n-\alpha)} \left(\frac{d}{dx}\right)^n \int_a^x \frac{f(\tau)d\tau}{(x-\tau)^{\alpha-n+1}},$$

where  $n = [\alpha] + 1$ ,  $[\alpha]$  means the integer part of  $\alpha$ .

**Definition 2** ([30, 36]). *The left fractional derivative in the sense of Caputo  ${}^C D_{[a,x]}^\alpha f(x)$  of order  $\alpha \in \mathbb{R}_+$  is defined by*

$${}^C D_{[a,x]}^\alpha f(x) = \frac{1}{\Gamma(n-\alpha)} \int_a^x \frac{f^{(n)}(\tau)d\tau}{(x-\tau)^{\alpha-n+1}}.$$

**Remark 1.** *Another definition of the Caputo fractional derivatives is via the Riemann-Liouville fractional derivative, which defined by*

$${}^C D_{[a,x]}^\alpha f(x) = D_{[a,x]}^\alpha \left[ f(x) - \sum_{k=0}^{n-1} \frac{f^{(k)}(a)}{k!} (x-a)^k \right].$$

In particular, when  $0 < \alpha < 1$  and  $a = 0$ , then  ${}^C D_{[0,x]}^\alpha f(x) = D_{[0,x]}^\alpha (f(x) - f(0))$ .

In order to integrate by an order  $\alpha \in \mathbb{R}^+$ , we present the fractional integral in the sense of Riemann-Liouville.

**Definition 3.** *The fractional integral in the sense of Riemann-Liouville is defined by*

$$I_{[a,x]}^\alpha f(x) = \frac{1}{\Gamma(\alpha)} \int_a^x (x-t)^{\alpha-1} f(t)dt. \tag{4}$$

**Remark 2.** • *An interesting propositionerty of the fractional Riemann-Liouville is*

$$I_{[a,x]}^\alpha D_{[a,x]}^\alpha f(x) = f(x), \tag{5}$$

when  $0 < \alpha < 1$  and  $f \in AC([a, b])$ .

- *We can deduce from the above equality that if  $0 < \alpha < 1$ ,  $a = 0$  and  $f \in AC([a, b])$  then:*

$$I_{[0,x]}^\alpha ({}^C D_{[0,x]}^\alpha f(x)) = f(x) - f(0). \tag{6}$$

In the case of the fractional derivative including the Caputo sense, the Leibniz (chain) rule is not verified. To remedy this problem, we will use the following theorem [1].

**Theorem 1.** suppose that  $\alpha \in (0, 1)$ ,  $\mathcal{H}$  is an Hilbert space, and  $w : [0, T] \rightarrow \mathcal{H}$  is such that  $\|w(t)\|_{\mathcal{H}}^2$  is absolutely continuous. Then it holds that

$${}_0^C D_t^\alpha \|w(t)\|_{\mathcal{H}}^2 \leq 2(w(t), {}_0^C D_t^\alpha w(t))_{\mathcal{H}},$$

for almost every  $t \in [0, T]$ .

Now we are in a situation to explain the solution to our problem.

**Definition 4.** We call  $u$  a weak solution of the proposed problem (3) if it satisfies

$$u \in L^2((0, T); H^2(\Omega)) \text{ and } \frac{\partial^\alpha u}{\partial t} \in L^2((0, T); H^2(\Omega)'),$$

such that

$$\left\{ \begin{array}{l} \left\langle \frac{\partial^\alpha u}{\partial t}, \varphi \right\rangle_{H^2(\Omega)', H^2(\Omega)} + \varepsilon \int_{\Omega} \mathcal{A}_u \nabla^2 u \cdot \nabla^2 \varphi dx - \frac{1}{\varepsilon} \int_{\Omega} \Delta(F'(u)) \varphi dx + \int_{\Omega} \lambda_D (u - f) \varphi dx = 0, \\ \forall \varphi \in L^2((0, T), H^2(\Omega)). \end{array} \right. \quad (7)$$

The following lemma gives a priori estimations of the solution  $u$  in (3).

**Lemma 1.** Let  $u$  be a weak solution of (3). Then there exists a constant  $C > 0$  such that

$$\|u\|_{L^\infty((0, T), L^2(\Omega))} + \|u\|_{L^2((0, T), H^2(\Omega))} + \left\| \frac{\partial^\alpha u}{\partial t} \right\|_{L^2((0, T), H^2(\Omega)')} \leq C.$$

*Proof.* We start by replacing  $\varphi = u$  in the variational problem (7) that gives

$$\left\langle \frac{\partial^\alpha u}{\partial t}, u \right\rangle_{H^2(\Omega)', H^2(\Omega)} + \varepsilon \int_{\Omega} \mathcal{A}_u \nabla^2 u \cdot \nabla^2 u dx - \frac{1}{\varepsilon} \int_{\Omega} \Delta(F'(u)) u dx + \int_{\Omega} \lambda_D (u - f) u dx = 0.$$

This implies

$$\left\langle \frac{\partial^\alpha u}{\partial t}, u \right\rangle_{H^2(\Omega)', H^2(\Omega)} + \varepsilon \int_{\Omega} \mathcal{A}_u |\nabla^2 u|^2 dx + \frac{1}{\varepsilon} \int_{\Omega} F''(u) |\nabla u|^2 dx + \int_{\Omega \setminus D} \lambda (u - f) u dx = 0.$$

Using

- Theorem 1, for the time fractional term derivative,
- the coercivity of  $\mathcal{A}_u$ , for some constant  $\nu$ ,
- $F''(\xi) \geq \gamma \xi^2 - C$ , for all  $\xi$ , for some constants  $\gamma$  and  $C$ ,

we have

$$\frac{1}{2} \frac{\partial^\alpha}{\partial t} \|u\|_{L^2(\Omega)}^2 + \nu \varepsilon \|\nabla^2 u\|_{L^2(\Omega)}^2 + \frac{\gamma}{\varepsilon} \int_{\Omega} u^2 |\nabla u|^2 dx + \int_{\Omega \setminus D} \lambda (u - f) u dx \leq \frac{C}{\varepsilon} \int_{\Omega} |\nabla u|^2 dx. \quad (8)$$

Also by Lemma 5.2 in [11], we have

$$\int_{\Omega} u^2 |\nabla u|^2 dx \geq C \int_{\Omega} u^4 dx - C \int_{\Omega} |\nabla u|^2 dx - C. \quad (9)$$

By the Holder's inequality,

$$\int_{\Omega} u^4 dx \geq C \left( \int_{\Omega} u^2 dx \right)^2, \quad (10)$$

and we now use the standard interpolation inequality, for an arbitrarily small constant  $\delta > 0$  that gives

$$\int_{\Omega} |\nabla u|^2 dx \leq \delta \int_{\Omega} (\Delta u)^2 dx + C(\delta) \int_{\Omega} u^2 dx \leq C(\delta) \int_{\Omega} u^2 dx.$$

Combining the last inequality, (9), (10) and absorbing the  $\varepsilon$  and  $\gamma$  into the constant  $C$ , we can rewrite inequality (8) as

$$\frac{1}{2} \frac{\partial^\alpha}{\partial t} \|u\|_{L^2(\Omega)}^2 + \nu \varepsilon \|\nabla^2 u\|_{L^2(\Omega)}^2 + \int_{\Omega \setminus D} \lambda (u - f) u dx \leq -C \left( \int_{\Omega} u^2 dx \right)^2 + C(\delta) \int_{\Omega} u^2 dx + C. \quad (11)$$

Using the fact that

$$\lambda \int_{\Omega \setminus D} u f dx - \lambda \int_{\Omega \setminus D} u^2 dx \leq \frac{\lambda}{2} \int_{\Omega \setminus D} f^2 dx - \frac{\lambda}{2} \int_{\Omega \setminus D} u^2 dx,$$

Eq. (11) becomes

$$\frac{1}{2} \frac{\partial^\alpha}{\partial t} \|u\|_{L^2(\Omega)}^2 + \nu \varepsilon \|\nabla^2 u\|_{L^2(\Omega)}^2 + \frac{\lambda}{2} \int_{\Omega \setminus D} f^2 dx \leq -C \left( \int_{\Omega} u^2 dx \right)^2 + C(\delta) \int_{\Omega} u^2 dx + C. \quad (12)$$

Now, let  $\zeta := \int_{\Omega} u^2 dx$ . Then the right-hand side of (12) is  $-C\zeta^2 + C(\delta)\zeta + C$  for some positive constants  $C$  depending on  $\delta$ . This is a parabola opening downwards and therefore is bounded from above by a constant which we denote it again as  $C$ . We integrate by order  $\alpha$  (see (4)) for  $s \in (0, \tau)$ , where  $\tau \in (0, T]$ , by using (6) in remark (2), (12) becomes

$$\frac{1}{2} \|u(\tau)\|_{L^2(\Omega)}^2 + \frac{\nu \varepsilon}{\Gamma(\alpha)} \int_0^\tau (\tau - s)^{\alpha-1} \|\nabla^2 u\|_{L^2(\Omega)}^2 ds + \frac{\lambda}{2\Gamma(\alpha)} \int_0^\tau \int_{\Omega \setminus D} (\tau - s)^{\alpha-1} f^2 dx ds \leq C + \frac{1}{2} \|f\|_{L^2(\Omega)}^2.$$

We have  $s \in (0, \tau)$  and  $\tau \in (0, T]$ , which implies  $(\tau - s) \leq \tau \leq T$ . Then, for  $0 < \alpha < 1$ , one has

$$(\tau - s)^{\alpha-1} \geq T^{\alpha-1},$$

which further implies

$$\frac{1}{2} \|u(\tau)\|_{L^2(\Omega)}^2 + \frac{\nu \varepsilon T^{\alpha-1}}{\Gamma(\alpha)} \int_0^\tau \|\nabla u\|_{L^2(\Omega)}^2 ds + \frac{\lambda T^{\alpha-1}}{2\Gamma(\alpha)} \int_0^\tau \int_{\Omega \setminus D} f^2 dx ds \leq C + \frac{1}{2} \|f\|_{L^2(\Omega)}^2.$$

We conclude that

$$\|u\|_{L^\infty((0,T),L^2(\Omega))} + \|u\|_{L^2((0,T),H^2(\Omega))} \leq C.$$

Now, we estimate the term  $\frac{\partial^\alpha u}{\partial t}$ . According to the variational formulation (7), we have

$$\left| \left\langle \frac{\partial^\alpha u}{\partial t}, \varphi \right\rangle_{H^2(\Omega)', H^2(\Omega)} \right| = \left| -\varepsilon \int_{\Omega} \mathcal{A}_u \nabla^2 u \cdot \nabla^2 \varphi dx + \frac{1}{\varepsilon} \int_{\Omega} \Delta(F'(u)) \varphi dx + \int_{\Omega} \lambda_D (f - u) \varphi dx \right|.$$

Using Holder inequality, we obtain

$$\begin{aligned} \left| \left\langle \frac{\partial^\alpha u}{\partial t}, \varphi \right\rangle_{H^2(\Omega)', H^2(\Omega)} \right| &\leq \varepsilon \|\mathcal{A}_u\|_{L^\infty(\Omega)} \|\nabla^2 u\|_{L^2(\Omega)} \|\nabla^2 \varphi\|_{L^2(\Omega)} \|\nabla \varphi\|_{L^2(\Omega)} \\ &\quad + \frac{1}{\varepsilon} \|F''(u)\|_{L^\infty(\Omega)} \|\nabla u\|_{L^2(\Omega)} + \lambda \|f - u\|_{L^2(\Omega)} \|\varphi\|_{L^2(\Omega)}. \end{aligned}$$

However, since  $\|\nabla \varphi\|_{L^2(\Omega)} \leq \|\varphi\|_{H^2(\Omega)}$  and  $\|\nabla^2 \varphi\|_{L^2(\Omega)} \leq \|\varphi\|_{H^2(\Omega)}$ , we have

$$\sup_{\varphi} \frac{\left| \left\langle \frac{\partial^\alpha u}{\partial t}, \varphi \right\rangle_{H^2(\Omega)', H^2(\Omega)} \right|}{\|\varphi\|_{H^2(\Omega)}} \leq \varepsilon \|\mathcal{A}_u\|_{L^\infty(\Omega)} \|\nabla^2 u\|_{L^2(\Omega)} + \frac{1}{\varepsilon} \|F''(u)\|_{L^\infty(\Omega)} \|\nabla u\|_{L^2(\Omega)} + \lambda \|f - u\|_{L^2(\Omega)}.$$

Then, we find

$$\left\| \frac{\partial^\alpha u}{\partial t} \right\|_{L^2((0,T), H^1(\Omega)')} \leq C,$$

which ends the proof. □

### 2.2 The main theorem

In this section, we present the existence result of a solution  $u$  in our model (3).

**Theorem 2.** *Let  $f \in L^2(\Omega)$ ,  $0 < \alpha < 1$ ,  $\rho \geq 0$  and  $\sigma, T > 0$ . Under the above assumptions, there exists a solution  $u$  of the problem (3), where  $u \in L^2((0, T); H^2(\Omega))$ .*

*Proof.* We prove the existence by using the fixed point theorem of Schauder [38]. For this reason, we introduce the following functional space

$$\mathcal{F}(0, T) = \left\{ w \in L^2((0, T); H^2(\Omega)); \frac{\partial^\alpha w}{\partial t} \in L^2((0, T); H^2(\Omega)') \right\}.$$

The  $\mathcal{F}(0, T)$  is an Hilbert space equipped with the norm

$$\|w\|_{\mathcal{F}(0,T)} = \|w\|_{L^2((0,T); H^2(\Omega))} + \left\| \frac{\partial^\alpha w}{\partial t} \right\|_{L^2((0,T); H^2(\Omega)')}.$$

Let  $w$  be in  $\mathcal{F}(0, T) \cap L^\infty((0, T); L^2(\Omega))$ , such that  $\|w\|_{L^\infty((0,T); L^2(\Omega))} \leq \|f\|_{L^2(\Omega)}$ . We define the variational problem associated to (3), and we fix a  $w$  in the nonlinear term of diffusion

$$\begin{aligned} \left\langle \frac{\partial^\alpha u}{\partial t}, Y \right\rangle_{H^2(\Omega)', H^2(\Omega)} + \varepsilon \int_{\Omega} \mathcal{A}_w \nabla^2 u \cdot \nabla^2 Y dx - \frac{1}{\varepsilon} \int_{\Omega} \Delta(F'(u)) Y dx + \int_{\Omega} \lambda_D (u - f) Y dx = 0, \\ \forall Y \in H^2(\Omega), \text{ a.e in } [0, T]. \end{aligned}$$

Using the results in Theorem 3.8 in [32], on the existence of parabolic equations, we can prove that the above problem admits a unique solution  $u_w$  in  $\mathcal{F}(0, T)$ , which satisfy the following estimations

$$\begin{cases} \|u_w\|_{L^2((0,T); H^2(\Omega))} \leq c_1, \\ \|u_w\|_{L^\infty((0,T); L^2(\Omega))} \leq \|f\|_{L^2(\Omega)}, \\ \left\| \frac{\partial^\alpha u_w}{\partial t} \right\|_{L^2((0,T); H^2(\Omega)')} \leq c_2, \end{cases}$$

where the constants  $c_1$  and  $c_2$  depends on  $\rho$ ,  $\sigma$  and  $f$ . The above estimations give us the right to define the subset  $\mathcal{F}_0$  of  $\mathcal{F}(0, T)$  as

$$\mathcal{F}_0 = \left\{ w \in \mathcal{F}(0, T), w(0) = f; \|w\|_{L^2((0, T); H^2(\Omega))} \leq c_1, \right. \\ \left. \|w\|_{L^\infty((0, T); L^2(\Omega))} \leq \|f\|_{L^2(\Omega)}, \left\| \frac{\partial^\alpha w}{\partial t} \right\|_{L^2((0, T); H^2(\Omega)')} \leq c_2 \right\}. \tag{13}$$

Let  $V : w \rightarrow V(w) = u_w$  be a mapping from  $\mathcal{F}_0$  to  $\mathcal{F}_0$ . It is clear that  $\mathcal{F}_0$  is a non empty, convex and weakly compact subspace of  $\mathcal{F}(0, T)$  (see [16]). To apply the Schauder Fixed-Point Theorem, we must prove that the mapping  $w \rightarrow V(w)$  is weakly continuous. For that reason, let  $(w_n)_n$  be a sequence which converges weakly to  $w \in \mathcal{F}_0$ . For simplicity reasons, we note  $u_n = V(w_n)$ . Using the compact inclusions of Sobolev spaces [2], the recent results of compactness on the fractional version of Aubin-Lions in [29] and by the estimations in (13), there exists a subsequence noted also  $(w_n)$  and  $(u_n)$  such that

$$\begin{aligned} \frac{\partial^\alpha u_n}{\partial t} &\rightharpoonup \frac{\partial^\alpha u}{\partial t} \quad \text{in } L^2((0, T); H^2(\Omega)'), \\ u_n &\rightarrow u \quad \text{in } L^2((0, T); L^2(\Omega)), \\ \nabla^2 u_n &\rightharpoonup \nabla^2 u \quad \text{in } (L^2((0, T); L^2(\Omega)))^2, \\ w_n &\rightarrow w \quad \text{in } L^2((0, T); L^2(\Omega)), \\ \mathcal{A}_{w_n} &\rightarrow \mathcal{A}_w \quad \text{in } L^2((0, T); L^2(\Omega)), \\ u_n(0) &\rightarrow f \quad \text{in } L^2(\Omega). \end{aligned}$$

As  $n \rightarrow +\infty$ , we obtain  $u = u_w = V(w)$ . By the uniqueness of the solution of (3), the sequence  $u_n = V(w_n)$  converges to  $u = V(w)$ , which proves the continuity of the mapping  $V$ . Finally, from the Schauder Fixed-Point Theorem, there exists a function  $w \in \mathcal{F}_0$  such that  $w = V(w) = u_w$ , which end the proof.  $\square$

### 3 Discretization, results and discussions

#### 3.1 Discretization of our model

Let  $\Omega(x_i, y_j)$  be the spatial partition of the image  $u$  for all  $i = 1, \dots, N$  and  $j = 1, \dots, M$ . We denote by  $u_{i,j}$  the value of  $u$  at the inner point  $(i, j)$ . Let  $\tau$  be the time step, i.e.  $t_0 = 0$ ,  $t_{k_{max}} = T$  and  $t_k = k \times \tau$  for  $k = 1, 2, \dots, (T_{max} - 1)$ . The Caputo fractional derivative of  $u$  at the inner point  $(i, j)$  is approached by [33]

$$\frac{\partial^\alpha u_{i,j}^k}{\partial t^\alpha} \approx \sigma_{\alpha, \tau} \sum_{l=1}^k \omega_l^{(\alpha)} \left( u_{i,j}^{k-l+1} - u_{i,j}^{k-l} \right) = \sigma_{\alpha, \tau} \left[ u_{i,j}^k - \sum_{l=1}^{k-1} \left( \omega_l^{(\alpha)} - \omega_{l+1}^{(\alpha)} \right) u_{i,j}^{k-l} - \omega_k^{(\alpha)} u_{i,j}^0 \right], \tag{14}$$

where

$$\sigma_{\alpha, \tau} = \frac{\tau^{-\alpha}}{\Gamma(2-\alpha)}, \quad \omega_l^{(\alpha)} = l^{1-\alpha} - (l-1)^{1-\alpha}, \quad \text{and } 1 = \omega_1^{(\alpha)} > \omega_2^{(\alpha)} > \dots > \omega_k^{(\alpha)}.$$

Now, we manage to implement a specific fast solver known as convexity splitting [26, 40]. Additionally, this method divides the energy functional of the proposed equation into two parts: a convex functional

plus a concave functional. The part of the Euler-Lagrange equation derived from convex part is implicitly dealt with in the numerical scheme, while the concave part is treated explicitly. The original Cahn-Hilliard equation (1) (with  $\lambda = 0$ ) is a gradient flow, i.e., we obtain the equation (1) by using an  $H^{-1}$  norm for the energy

$$E_1 = \int_{\Omega} \frac{\varepsilon}{2} |\nabla u|^2 + \frac{1}{\varepsilon} F(u) dx, \tag{15}$$

with the fidelity term under an  $L^2$  norm for the energy

$$E_2 = \lambda_0 \int_{\Omega \setminus D} (f - u)^2 dx. \tag{16}$$

However, the functional  $E_1$  is not like ours, precisely in the first term. The new functional  $E_1$  applied to our model has the following form

$$E_1^+ = \int_{\Omega} \frac{\varepsilon}{2} |\mathcal{A}_v \nabla u|^2 + \frac{1}{\varepsilon} F(u) dx, \tag{17}$$

where  $v = f$  at the first iteration.

Our model (3) (or the modified Cahn-Hilliard equation in general) is neither a gradient flow in  $H^{-1}$ -norm nor in  $L^2$ -norm. But, the basic idea of our implementation method, convexity splitting, is that the one for the Cahn-Hilliard energy  $E_1^+$  in Eq. (17) and the one for the energy  $E_2$  in Eq. (16), can still be applied to our approach with good results. For example, for some positive constants  $C_1$  and  $C_2$ , we split  $E_1^+$  as  $E_1^+ = E_{11} - E_{12}$ , where

$$E_{11} = \int_{\Omega} \frac{\varepsilon}{2} |\mathcal{A}_v \nabla u|^2 + \frac{C_1}{2} |u|^2 d\text{vec}x,$$

and

$$E_{12} = \int_{\Omega} -\frac{1}{\varepsilon} F(u) + \frac{C_1}{2} |u|^2 d\text{vec}x.$$

Similarly for  $E_2$

$$E_2 = E_{21} - E_{22},$$

where

$$E_{21} = \int_{\Omega \setminus D} \frac{C_2}{2} |u|^2 d\text{vec}x,$$

and

$$E_{22} = \int_{\Omega \setminus D} -\lambda_0 (f - u)^2 + \frac{C_2}{2} |u|^2 d\text{vec}x.$$

Using the discrete form of the time-fractional derivative discussed above in (14), we present the resulting scheme

$$\frac{\partial^\alpha u^k}{\partial t^\alpha} = -\nabla_{H^{-1}} \left( E_{11}^k - E_{12}^{k-1} \right) - \nabla_{L^2} \left( E_{21}^k - E_{22}^{k-1} \right), \tag{18}$$

where  $\nabla_{H^{-1}}$  and  $\nabla_{L^2}$  are respectively the gradient descent with respect to the  $H^{-1}$  inner product, and  $L^2$  inner product. We rewrite (18) at the inner point  $(i, j)$  as follows

$$\begin{aligned} \sigma_{\alpha, \tau} \left[ u_{i,j}^k - \sum_{l=1}^{k-1} \left( \omega_l^{(\alpha)} - \omega_{l+1}^{(\alpha)} \right) u_{i,j}^{k-l} - \omega_k^{(\alpha)} u_{i,j}^0 \right] &+ \varepsilon \nabla^2 \cdot (\mathcal{A}_{u_{i,j}^k} \nabla^2 u_{i,j}^k) - C_1 \Delta u_{i,j}^k + C_2 u_{i,j}^k \\ &= \Delta \left( \frac{1}{\varepsilon} F' \left( u_{i,j}^{k-1} \right) \right) + \lambda_D \left( f_{i,j} - u_{i,j}^{k-1} \right) - C_1 \Delta u_{i,j}^{k-1} + C_2 u_{i,j}^{k-1}, \end{aligned}$$

which implies

$$\begin{aligned}
 u_{i,j}^k + \frac{1}{\sigma_{\alpha,\tau}} \left[ \varepsilon \nabla^2 \cdot (\mathcal{A}_{u_{i,j}^k} \nabla^2 u_{i,j}^k) - C_1 \Delta u_{i,j}^k + C_2 u_{i,j}^k \right] &= \sum_{l=1}^{k-1} \left( \omega_l^{(\alpha)} - \omega_{l+1}^{(\alpha)} \right) u_{i,j}^{k-l} \\
 + \omega_k^{(\alpha)} u_{i,j}^0 + \frac{1}{\sigma_{\alpha,\tau}} \left[ \Delta \left( \frac{1}{\varepsilon} F' \left( u_{i,j}^{k-1} \right) \right) + \lambda_D \left( f_{i,j} - u_{i,j}^{k-1} \right) - C_1 \Delta u_{i,j}^{k-1} + C_2 u_{i,j}^{k-1} \right], & \quad (19)
 \end{aligned}$$

for all  $k \geq 1$ .

The final discrete equation (19) can be solved, at iteration  $u^k$  where  $u^{k-1}$  is given, with a two-dimensional Fast-Fourier Transform method, which already exists in Matlab.

Finally, we recall that the inpainting is performed in a two-step method. Firstly, the inpainting is done, taking a larger value of  $\varepsilon$ , which results a preservation and a reconnection of shapes with strong edges and corners displayed by our diffusion term. Secondly, we use the results of the first step but with a smaller value of  $\varepsilon$  in order to extract and sharpen the edge after the topological reconnection made by the function  $F'(u)$ . Before we give the numerical results, we introduce some useful discretization. We denote by  $(\partial_x u)_{i,j}$  (resp.  $(\partial_y u)_{i,j}$ ) the discretization of the operators  $\partial_x u$  (resp.  $\partial_y u$ ). They can be calculated as follows

$$\begin{aligned}
 (\partial_x u)_{i,j} &= \begin{cases} u_{i+1,j} - u_{i,j}, & \text{if } i < N, \\ 0, & \text{if } i = N, \end{cases} \\
 (\partial_y u)_{i,j} &= \begin{cases} u_{i,j+1} - u_{i,j}, & \text{if } j < M, \\ 0, & \text{if } j = M. \end{cases}
 \end{aligned}$$

For the second derivatives, we have

$$\begin{aligned}
 (\partial_{xx} u)_{i,j} &= \begin{cases} u_{i+1,j} - 2u_{i,j} + u_{i-1,j}, & \text{if } 1 < i < N, \\ u_{i+1,j} - u_{i,j}, & \text{if } i = 1, \\ u_{i-1,j} - u_{i,j}, & \text{if } i = N, \end{cases} \\
 (\partial_{yy} u)_{i,j} &= \begin{cases} u_{i,j+1} - 2u_{i,j} + u_{i,j-1}, & \text{if } 1 < j < M, \\ u_{i,j+1} - u_{i,j}, & \text{if } j = 1, \\ u_{i,j-1} - u_{i,j}, & \text{if } j = N, \end{cases} \\
 (\partial_{xy} u)_{i,j} &= \begin{cases} u_{i,j+1} - u_{i,j} + u_{i-1,j+1} + u_{i-1,j}, & \text{if } 1 < i < N, 1 < j < M, \\ 0, & \text{if } i = 1, \\ 0, & \text{if } i = N, \end{cases} \\
 (\partial_{yx} u)_{i,j} &= \begin{cases} u_{i+1,j} - u_{i,j} + u_{i+1,j-1} + u_{i,j-1}, & \text{if } 1 < i < N, 1 < j < M, \\ 0, & \text{if } j = 1, \\ 0, & \text{if } j = M. \end{cases}
 \end{aligned}$$

### 3.2 Results and discussions

In this work, all our simulations were done by Matlab 2018, on a computer with a 3 GHz processor and 16 Gb of RAM. To test the performance of our approach, we use simulations starting with the Figures 1-3. We compare the results of inpainting of the masked binary image with an unknown center with

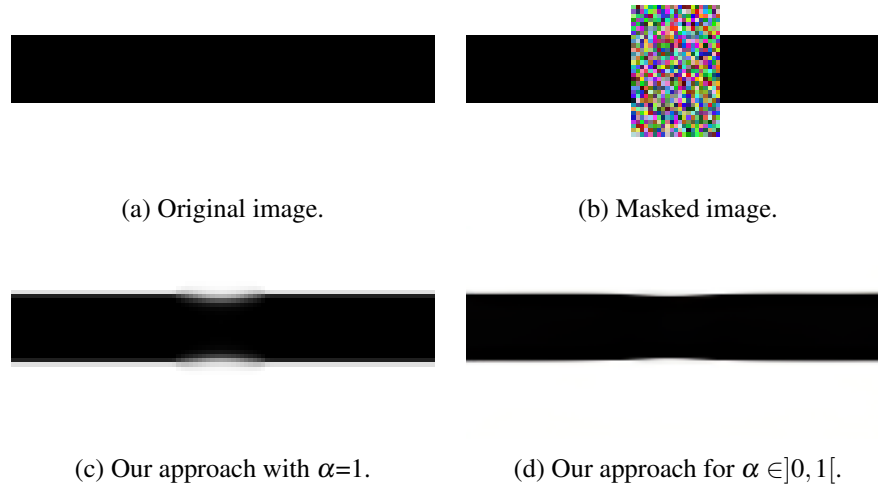


Figure 1: Binary image masked with an unknown center and our solutions.

our approach solutions. The first solution is when the fractional-time order  $\alpha$  equals 1 which coincides with the classical first derivative and when the fractional-time order  $\alpha$  belongs to  $]0, 1[$ , we take  $\alpha$  in the first set as 0.83. We take  $\lambda = 10^2$ . In those figures, we use a process with two-steps with an inpainting region with an added noise level. For example, in Figure 1 (a), we start running the term that contains the Cahn-Hilliard equation with a big value of  $\varepsilon = 0.9$ . We switch to a small value of  $\varepsilon = .01$ , using the result from the first step as initial data. The final result is reached and it is shown in the last image of every figure. In this first test, the time step  $\tau = 0.1$ . Similarly for the rest of numerical tests. Moreover,

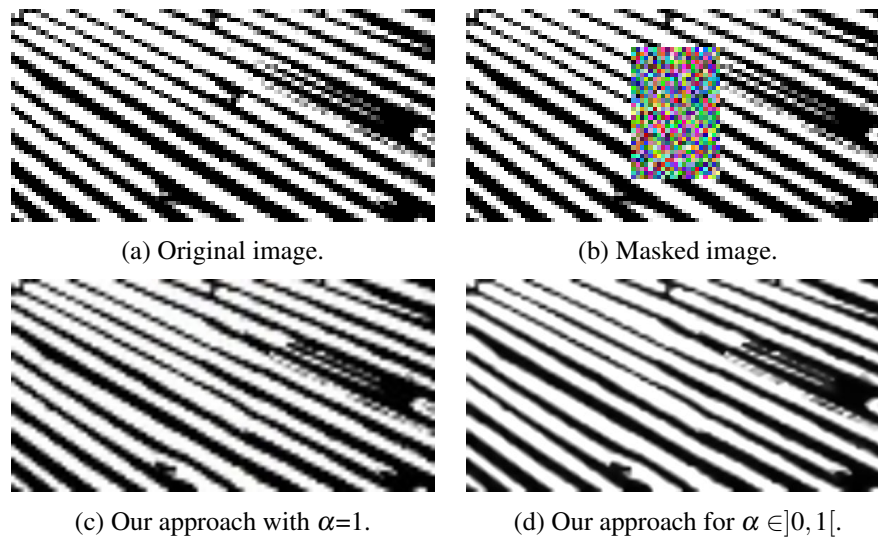


Figure 2: Binary image masked with an unknown center and our solution.

the propositionriety of memory effect potential can be seen clearly in our result images where  $\alpha \in ]0, 1[$ .

This potential is clear in all figures and especially in Figure 3, where the resulting image converges to the original one thanks to the memory effect potential contrarily to where  $\alpha = 1$  (classical derivative).

Additionally, it is clear that the preservation techniques obtained from the proposed model give sharpness to the edges and corners of the masked images, next to its reconnections. This later is very clear in the resulting images, where the strong and pointy edges and hard corners are recovered thanks to the diffusion operator utilized in our approach. Furthermore, a contour representation is also introduced in Figure 4, which shows the preserving quality of the proposed model in the case of  $\alpha \in ]0, 1[$ . The recovery of pointy edges and corners is successfully guaranteed thanks to the memory potential effect obtained from the Caputo fractional-time derivative. For more tests, we took a patch from an image. As Figure 5 shows, we take the intensity of pixels of the mentioned patch, to observe the behavior of the image in the presence of a mask and a small additive noise. It is obvious that the resulting images converge to the original ones, which shows that the recovery is robust by our approach. In the numerical simulations, we justified all the above assumptions and modeling choices, such as the memory effect produced by the time-fractional derivative (Caputo) and the features preservation guaranteed by the diffusion term (Weickert).

## 4 Conclusions

In this work, we manage to propose a modified version of the modified Cahn-Hilliard with a new diffusivity term and a time-fractional derivative over time (Caputo definition) to apply the memory effect potential. We provide an existence result, thanks to Schauder Fixed Point Theorem and some recent results on the fractional version of Aubin-Lions. The numerical simulations are made by the convexity splitting, and they justify the modeling choices we make during this paper (recovery and preservation). The resulting images are perfectly recovered, the sharpness of edges and corners is well preserved and the reconnection between the image features is obtained, thanks to the potential of memory effect and matrix diffusion term.

## Acknowledgements

We would like to thank the editor and anonymous reviewers for their helpful comments and valuable suggestions.

## References

- [1] A. Alikhanov, *A priori estimates for solutions of boundary value problems for fractional-order equations*, *Differ. Equ.* **46** (2010) 660–666.
- [2] H. Attouch, G. Buttazzo, G. Michaille, *Variational analysis in sobolev and bv spaces: applications to pdes and optimization*, SIAM, 2014.
- [3] A. Babaei, *Solving a time-fractional inverse heat conduction problem with an unknown nonlinear boundary condition*, *J. Math. Model.* **7** (2019) 85–106.
- [4] B. Beisner, D. Haydon, K. Cuddington, *Hysteresis*, *Encycl. Ecol.* (2008) 1930-1935.

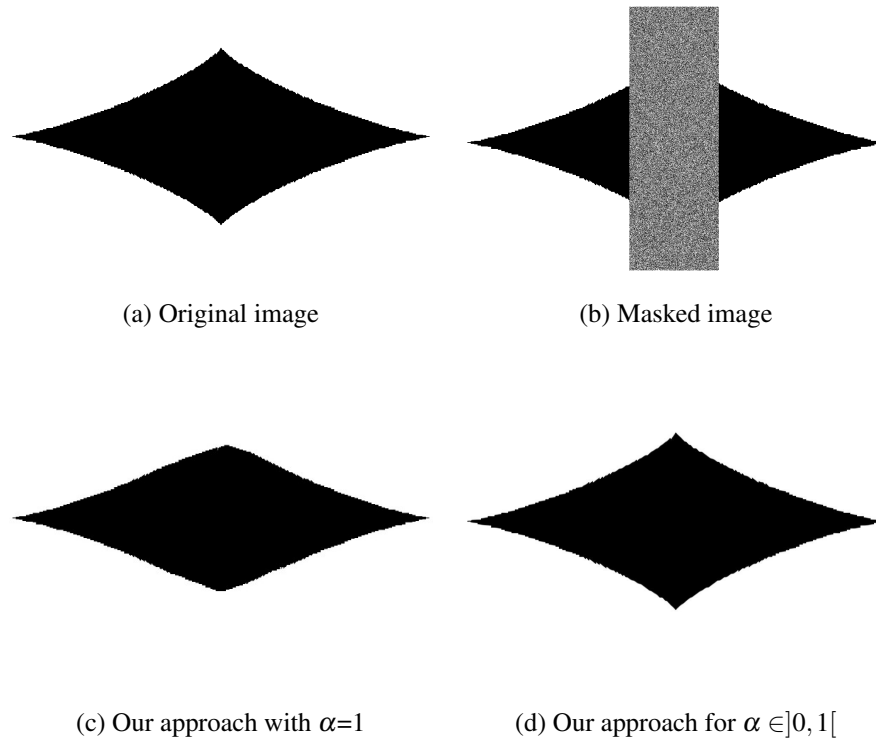


Figure 3: Binary image masked with an unknown center and our solution.

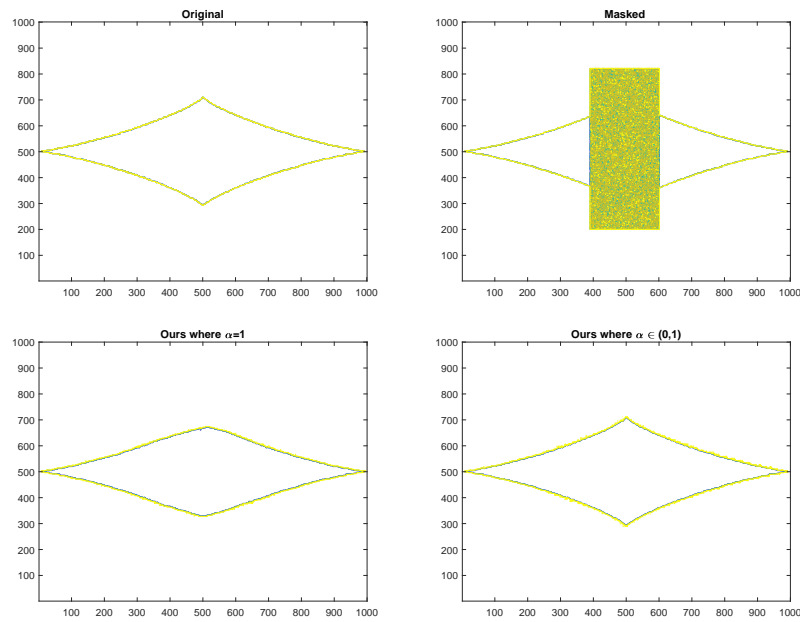
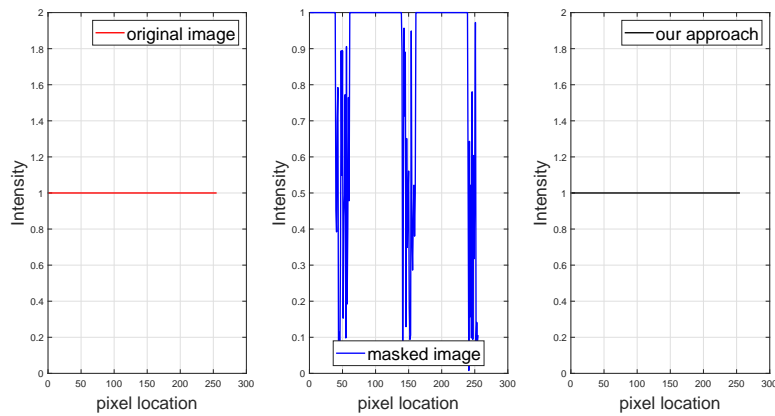
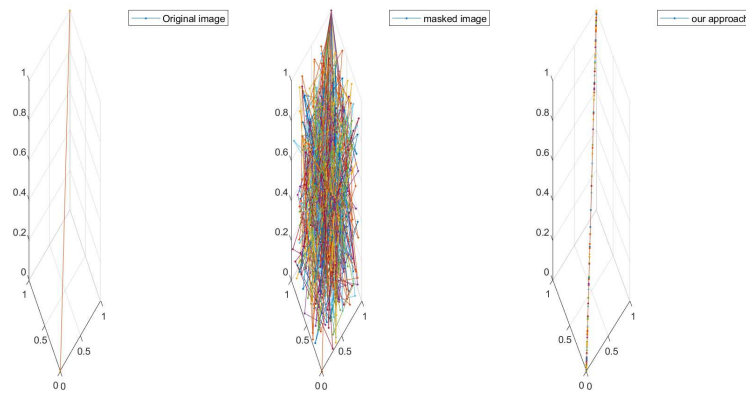


Figure 4: Contour presentations result for the third test image.



(a) The intensity of a patch in the original, masked and result images.



(b) The intensity of the original, masked and result images.

Figure 5: Intensity result for the first test image.

- [5] A. Ben-Loghfyry, A. Hakim, *Time-fractional diffusion equation for signal and image smoothing*, *Math. Model. Comput.* **9** (2022) 351–364.
- [6] A. Ben-loghfry, A. Hakim, *Reaction-diffusion equation based on fractional-time anisotropic diffusion for textured images recovery*, *Int. J. Comput. Math.* **8** (2022) 177.
- [7] A. Ben-loghfry, A. Hakim, *Robust time-fractional diffusion filtering for noise removal*, *Math. Methods Appl. Sci.* **45** (2022) 9719–9735.
- [8] A. Ben-Loghfyry, A. Hakim, A. Laghrib, *A denoising model based on the fractional beltrami regularization and its numerical solution*, *J. Appl. Math. Comput.* (2022) 1–33.
- [9] M. Bertalmio, A.L. Bertozzi, G. Sapiro, *Navier-stokes, fluid dynamics, and image and video inpainting*, *Proceedings of the 2001 IEEE Computer Society Conference on Computer Vision and Pattern Recognition. CVPR 2001*, vol. 1, IEEE, 2001, pp. I–I.

- [10] M. Bertalmio, G. Sapiro, V. Caselles, C. Ballester, *Image inpainting*, Proceedings of the 27th annual conference on Computer graphics and interactive techniques, (2000) 417–424.
- [11] A. Bertozzi, S. Esedoglu, A. Gillette, *Analysis of a two-scale cahn–hilliard model for binary image inpainting*, Multiscale Model. Simul. **6** (2007) 913–936.
- [12] A. Bertozzi, C.B. Schönlieb, *Unconditionally stable schemes for higher order inpainting*, Commun. Math. Sci. **9** (2011) 413–457.
- [13] A.L. Bertozzi, S. Esedoglu, A. Gillette, *Inpainting of binary images using the cahn–hilliard equation*, IEEE Trans. Image Process. **16** (2006) 285–291.
- [14] J.F. Blowey, C.M. Elliott, *The cahn–hilliard gradient theory for phase separation with non-smooth free energy part i: Mathematical analysis*, Eur. J. Appl. Math. **2** (1991) 233–280.
- [15] J.F. Blowey, C.M. Elliott, *The cahn–hilliard gradient theory for phase separation with non-smooth free energy part ii: numerical analysis*, Eur. J. Appl. Math. **3** (1992) 147–179.
- [16] H. Brezis, *Functional Analysis, Sobolev Spaces and Partial differential Equations*, Springer Science & Business Media, 2010.
- [17] M. Burger, L. He, C.B. Schönlieb, *Cahn–hilliard inpainting and a generalization for grayvalue images*, SIAM J. Imaging Sci. **2** (2009) 1129–1167.
- [18] J.W. Cahn, J.E. Hilliard, *Free energy of a nonuniform system. i. interfacial free energy*, Chem. Phys. **28** (1958) 258–267.
- [19] M. Caputo, W. Plastino, *Diffusion in porous layers with memory*, Geophys. J. Int. **158** (2004) 385–396.
- [20] L. Chen, F. Ghanbarnejad, D. Brockmann, *Fundamental properties of cooperative contagion processes*, New J. Phys. **19** (2017) 103041.
- [21] L. Cherfils, H. Fakh, A. Miranville, *A cahn–hilliard system with a fidelity term for color image inpainting*, J. Math. Imaging Vis. **54** (2016) 117–131.
- [22] L. Cherfils, H. Fakh, A. Miranville, *A complex version of the cahn–hilliard equation for grayscale image inpainting*, Multiscale Model. Simul. **15** (2017) 575–605.
- [23] H. El-Saka, *The fractional-order sir and sirs epidemic models with variable population size*, Math. Sci. Lett. **2** (2013) 195.
- [24] C.M. Elliott, *The Cahn-Hilliard Model for the Kinetics of Phase Separation, Mathematical Models for Phase Change Problems*, Springer, 1989.
- [25] S. Esedoglu, J. Shen, *Digital inpainting based on the mumford–shah–euler image model*, Eur. J. Appl. Math. **13** (2002) 353–370.
- [26] D.J. Eyre, *An unconditionally stable one-step scheme for gradient systems*, Unpublished article **6** (1998).

- [27] H. Garcke, K.F. Lam, V. Styles, *Cahn–hilliard inpainting with the double obstacle potential*, SIAM J. Imaging Sci. **11** (2018) 2064–2089.
- [28] A. Hakim, A. Ben-Loghfry, *A total variable-order variation model for image denoising*, AIMS Mathematics **4** (2019) 1320–1335.
- [29] L. Li, J.G. Liu, *Some compactness criteria for weak solutions of time fractional pdes*, SIAM J. Math. Anal. **50** (2018) 3963–3995.
- [30] J.T. Machado, V. Kiryakova, F. Mainardi, *Recent history of fractional calculus*, Commun. Nonlinear Sci. Numer. Simul. **16** (2011) 1140–1153.
- [31] E.M. Mendes, G.H. Salgado, L.A. Aguirre, *Numerical solution of caputo fractional differential equations with infinity memory effect at initial condition*, Commun. Nonlinear Sci. Numer. Simul. **69** (2019) 237–247.
- [32] J. Mu, B. Ahmad, S. Huang, *Existence and regularity of solutions to time-fractional diffusion equations*, Comput. Math. with Appl. **73** (2017) 985–996.
- [33] D.A. Murio, *Implicit finite difference approximation for time fractional diffusion equations*, Comput. Math. with Appl. **56** (2008) 1138–1145.
- [34] D.S. Oliveira, E.C. de Oliveira, *On a caputo-type fractional derivative*, Adv. Pure Appl. Math. **10** (2019) 81–91.
- [35] A. Pimenov, T.C. Kelly, A. Korobeinikov, M.J. OCallaghan, A.V. Pokrovskii, D. Rachinskii, *Memory effects in population dynamics: spread of infectious disease as a case study*, Math. Model. Nat. Phenom. **7** (2012) 204–226.
- [36] I. Podlubny, *Fractional Differential Equations: An Introduction to Fractional Derivatives, Fractional Differential Equations, to Methods of Their Solution and Some of Their Applications*, Elsevier, 1998.
- [37] M. Saeedian, M. Khalighi, N. Azimi-Tafreshi, G. Jafari, M. Ausloos, *Memory effects on epidemic evolution: The susceptible-infected-recovered epidemic model*, Phys. Rev. E **95** (2017) 022409.
- [38] J.T. Schwartz, H. Karcher, *Nonlinear Functional Analysis*, CRC Press, 1969.
- [39] J. Shen, T.F. Chan, *Mathematical models for local nontexture inpaintings*, SIAM J. Appl. Math. **62** (2002) 1019–1043.
- [40] B.P. Vollmayr-Lee, A.D. Rutenberg, *Fast and accurate coarsening simulation with an unconditionally stable time step*, Phys. Rev. E. **68** (2003) 066703.
- [41] T.K. Yamana, X. Qiu, E.A. Eltahir, *Hysteresis in simulations of malaria transmission*, Adv. Water Resour. **108** (2017) 416–422.
- [42] Q. Zou, *An image inpainting model based on the mixture of perona–malik equation and cahn–hilliard equation*, J. Appl. Math. Comput. **66** (2021) 21–38.